Synthesis of Amphiphilic Block Copolymers Based on *tert*-Butyl Methacrylate and 2-(*N*-Methylperfluorobutanesulfonamido)ethyl Methacrylate and Its Behavior in Water

K. Busse* and J. Kressler

Fachbereich Ingenieurwissenschaften, Martin-Luther-Universität Halle-Wittenberg,
D-06099 Halle (Saale), Germany

D. van Eck and S. Höring

Fachbereich Chemie, Martin-Luther-Universität Halle-Wittenberg, D-06099 Halle (Saale), Germany

Received September 26, 2001

ABSTRACT: Di- and triblock copolymers of *tert*-butyl methacrylate (tBMA) and 2-(*N*-methylperfluorobutanesulfonamido)ethyl methacrylate (FMA) were synthesized by sequential anionic polymerization. These polymers were characterized by size-exclusion chromatography and ^{1}H and ^{19}F NMR spectroscopy. The microphase separation of bulk samples was studied by atomic force microscopy and small-angle X-ray scattering. Thermal annealing of the block copolymers at 200 °C yielded inter- and intramolecular anhydrides due to the splitting of the ester having *tert*-butyl groups connected with isobutene formation. This conversion was followed by time-resolved Fourier transform infrared (FT-IR) spectroscopy. The anhydrides can be transformed into the sodium salt of methacrylic acid units in 1 N NaOH under reflux. The thermal ester splitting of the tBMA block at 200 °C did not influence the FMA block. The obtained block copolymers were soluble in water when the FMA content was less than 10 mol %. The behavior of these solutions was studied by various experimental methods. The critical micelle concentration was obtained by surface tension measurements. The micelle dimensions were determined by dynamic light scattering. The size and inner structure of the micelles were investigated by small-angle X-ray scattering and could also be observed by transmission electron microscopy after transfer of the diluted solutions onto carbon films. Typical polyelectrolyte effects were observed by viscosity measurements for PtBMA only. For block copolymers the aggregation behavior is dominating even at very low concentrations.

Introduction

Amphiphilic block copolymers are used nowadays for a broad variety of applications,[1−11] e.g., as reactors for nanoparticles, as thickening agents in paints, in cosmetics, for enhanced oil recovery etc. Hydrophobically modified water-soluble polymers (HMWSP) are gaining importance due to their unique rheological and structural properties. There are several possible ways to combine hydrophobic and hydrophilic blocks: by sequential anionic polymerization,[12,13] group transfer polymerization,[14,15] or cationic polymerization.[16−18] The water-soluble block can be formed, e.g., by ethylene oxide[12] or by polyelectrolytes.[19] There is a large variety of hydrophobic blocks ranging, e.g., from polystyrenes to poly(methacrylates) with long alkyl side chains. The strongest hydrophobic effect is obtained by perfluoroalkyl groups.[6,18] Until now most studies have been devoted to synthesis of such polymers by radical solution or bulk copolymerization in which the comonomer distribution in the chain is determined by reactivity ratios.[20,21] Only a few attempts have been reported to prepare fluorine-containing amphiphilic block copolymers with water-soluble blocks.[18,22−24]

The attention has been focused mainly on HMWSP, based on random copolymers or water-soluble polymers end-capped with hydrophobic groups. When these polymers are dissolved in water they may form aggregates, presumably of micellar type.[25−27] For diluted solutions the effect of single chains is dominating, whereas with increasing concentration the micelles and finally the gel characterize the physical behavior. The range of concentrations separating the lower limit where virtually single chains are dominating and the upper limit where virtually only micelles are present can be detected, e.g., by surface tension measurements. The extrapolated overlap concentration is called the critical micelle concentration (cmc)[28] or overlap concentration (c*). The c* value has a more general meaning as for different measurement methods the detected change in the behavior might be due to different physical reasons such as a change in surface covering or the formation of a transient network via association of the hydrophobic groups.

The shape of the micelles depends on the block lengths and the temperature. Spherical, oblate, and rodlike structures can be observed.[29−31] Generally, the hydrophobic (A) blocks build a core covered by a shell of the hydrophilic (B) parts in water. For ABA triblock copolymers, single chains may form loops (both ends belongs to the same micelle) or bridges (two micelles are connected).[32,33]

In this work sequential anionic polymerization is employed for the preparation of amphiphilic block copolymers. The hydrophobicity is introduced by a methacrylate with a perfluorinated side chain and the hydrophilic block is the sodium salt of poly(methacrylic acid) obtained by thermal annealing at 200 °C followed by alkaline treatment of the respective *tert*-butyl ester. By recording the ester splitting on a Fourier transform infrared (FT-IR) spectrometer it was possible to show

---

* To whom correspondence should be addressed: fax 49-3461-46-2592; e-mail karsten.busse@iw.uni-halle.de.

10.1021/ma0116809 CCC: $22.00

Chart 1. Comonomers

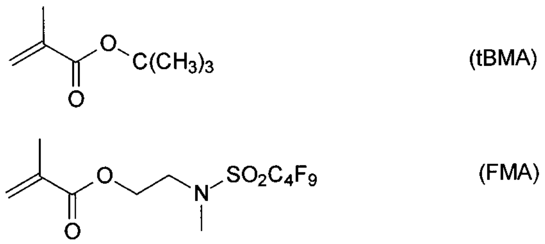

that the perfluorinated parts were not affected and the anhydride is built. It was known from literature[34] that the monomer *tert*-butyl methacrylate can be used for anionic polymerization and the ester group can easily be modified. The molecular parameters of the polymers are reported as well as the morphology formation in bulk. The solutions of the transformed (amphiphilic) block copolymers in water are characterized by surface tension measurements, rheology, transmission electron microscopy (TEM), small-angle X-ray scattering (SAXS), and dynamic light scattering. The first two methods were used to obtain information about c^*. Finally, the addition of colloidal gold particles is taken into consideration to get more information about micelle formation and stability.

Experimental Section

Materials. *tert*-Butyl methacrylate (tBMA, Polysciences Europe GmbH; Chart 1) was dried and distilled over CaH_2. Before use, it was condensed from $(C_2H_5)_3Al$ under vacuum according to the standard procedure.[35] 2-(*N*-Methylperfluorobutanesulfonamido)ethyl methacrylate (FMA; Chart 1) was kindly supplied by Bayer AG, recrystallized twice from methanol, and finally sublimated under high vacuum. Tetrahydrofuran (THF, Merck) was dried over CaH_2, distilled from the purple sodium salt of the benzophenone dianion, stored over K/Na alloy, and finally distilled from the alloy. Naphthalene potassium was prepared through the reaction between naphthalene (Fluka) and potassium (Merck) in THF at 0 °C.[36] 1,1-Diphenyl-3-methylpentyllithium was synthesized by reaction of 1,1-diphenylethylene (Merck) with *sec*-butyllithium (Merck; dissolved in cyclohexane) at 25 °C just before the polymerization.

Polymerizations. All polymerizations were carried out at −78 °C. The reaction components were added to a previously flamed and argon-purged glass reactor. At first the THF (only in FMA homopolymerization after preaddition of LiCl[37]) and a solution of the initiator in THF were filled into the reactor through a rubber septum with a stainless steel capillary followed by dropwise addition of the calculated amount of the first monomer, tBMA. After being stirred for 1 h, a prechilled THF solution of the second monomer (FMA) was added. The reaction was allowed to last 9 h and then stopped with methanol/water. The polymer was isolated by precipitation in methanol.

SEC Measurements. For determination of molar masses and molar mass distribution, the samples were prepared by dissolving the purified polymer in HPLC-grade THF. The size-exclusion chromatography (SEC) was performed in THF at 25 °C on a Knauer chromatograph equipped with styragel columns and refractive index detector at a flow rate of 1.0 mL/min. Poly(methyl methacrylate) standards from Polymer Standard Service were used for calibration.

Fluorine-19 and Proton NMR Measurements. ^1H and ^{19}F NMR spectra were recorded on a Varian spectrometer operating at 300 MHz in $CDCl_3$ at 25 °C.

Preparation of Water-Soluble Polymers. A selective two-step transformation of the tBMA block into the water-soluble sodium salt of poly(methacrylic acid) was carried out. The thermal ester splitting (in anhydride, isobutene, and water) of the tBMA units was performed at 200 °C under vacuum.[38] The reactions were recorded with an FT-IR spectrometer (Bruker IFS 88). To convert the anhydride-containing blocks into the sodium salt of methacrylic acid, the samples (1−2 g) were refluxed for 1 h with 1 N NaOH. The gellike solutions were purified by dialysis against deionized water, using a dialysis membrane tube (Nadir, pore size 2.5−3 nm), and then filtered with a 0.8 μm CA membrane filter (Rotilabo). The solid polymer obtained by evaporation of the solvent was dried at 40 °C in a vacuum oven and dissolved in deionized water for subsequent measurements.

Atomic Force Microscopy (AFM). Measurements were carried out with a Nanoscope IIIa AFM (Digital Instruments). The tapping mode was applied. The polymer was dissolved in 2,2,3,3-tetrafluoro-1-propanol or THF and a film was formed by slow evaporation of the solvent at ambient temperature.

Transmission Electron Microscopy (TEM). A Zeiss CEM902 was used with an acceleration voltage of 80 kV. The samples for TEM were dissolved in water and in some cases colloidal gold was added. The solutions were cast onto copper grids covered with a carbon film.

Small-Angle X-ray Scattering (SAXS). SAXS measurements were performed in an evacuated Kratky compact camera (Anton Paar K. G.) with an 80 μm entrance slit. Cu K_α radiation with a wavelength of $\lambda = 0.154$ nm was used. The scattered intensity, *I*, was recorded by a scintillation counter in a step-scanning mode at room temperature. The scattering profiles were corrected for background scattering and desmeared.[39] The cosine Fourier transformation of the scattering curve yields the linear correlation function $K(z)$ defined by[40]

$$K(z) = \int_0^\infty 4\pi s^2 I(s) \cos(2\pi s z)\, ds \qquad (1)$$

s is the scattering vector [$s = 2 \sin(\theta)/\lambda$].

Dynamic Light Scattering (DLS). The experimental equipment consisted of a DLS−SLS 5000 laser light scattering goniometer (ALV Langen, Germany), equipped with a 140 mW Nd:YAG laser (diode-pumped, frequency-doubled; ADLAS Lübeck, Germany) with a wavelength of 532 nm, and a ALV-5000 multiple τ digital correlator. The scattered light was detected at an angle of 90° and the measurements were carried out at $T = 25$ °C. The samples were held in a cylindrical glass vessel. The pair correlation function $g^2(t)$ obtained by dynamic light scattering is analyzed to get effective diffusion coefficients D_{eff} of the samples. The hydrodynamic radius of assumed hard spheres is calculated via the Stokes−Einstein equation $r_{\mathrm{hyd}} = kT/(6\pi\eta D_{\mathrm{eff}})$, where k is the Boltzmann constant and η is the viscosity of the solvent at temperature T.

Rheology and Wilhelmy Plate Method. The relative viscosities were determined by using a capillary viscometer (capillary diameter 0.6 mm). The measurements were carried out at 25 °C. For surface tension measurements at 25 °C, a digital tensiometer K10T (Krüss), equipped with a platinum plate, was used.

Results and Discussion

The synthesis is outlined in Figure 1. The first step is the block copolymerization of tBMA and FMA, which is done for various FMA contents between 1 and 38 mol %. In addition, two homopolymers of PtBMA and PFMA are synthesized. Table 1 contains the conditions and results of homopolymerizations and block copolymerizations.

All the samples have small molar mass distributions determined by SEC measurements in THF with poly(methyl methacrylate) standards. The calculated values for M_w/M_n are below 1.2 as expected for a living anionic polymerization.[41] The relative FMA contents are determined by ^{19}F and ^1H NMR measurements. To verify that block copolymers are formed, it is necessary to demonstrate a microphase separation of the respective blocks.

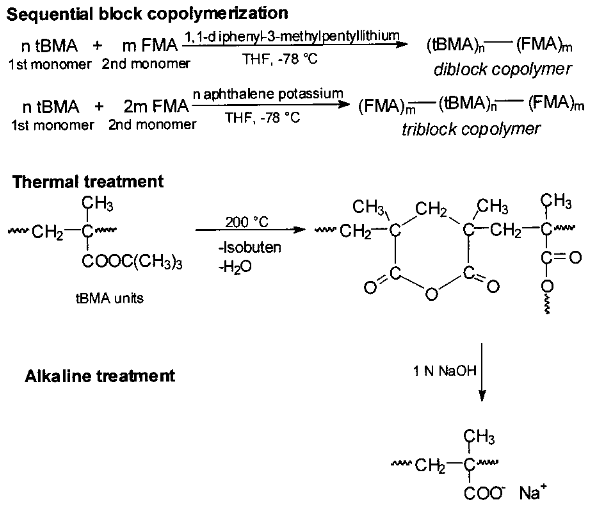

Figure 1. Scheme of the synthesis of amphiphilic block copolymers.

Table 1. Homopolymerization and Block Copolymerization of tBMA and FMA at − 78 °C in THF

sample code	M_n[a] (kg/mol)	M_w/M_n[a]	FMA[b] (mol %)
PtBMA-1[c]	90.1	1.08	0
PtBMA-2[c]	71.9	1.13	0
Di-1[d]	30.9	1.06	2
Tri-1[c]	57.1	1.15	1
Tri-2[c]	54.4	1.19	3
Tri-3[c]	51.7	1.10	7
Tri-4[c]	56.7	1.10	7
Tri-5[c]	57.0	1.09	8
Tri-6[c]	72.4	1.12	26
Tri-7[c]	49.4	1.15	38
PFMA-1[e]	3.1	1.03	100
PFMA-2[e]	13.2	1.10	100

[a] Determined by SEC in THF, with poly(methyl methacrylate) standards. [b] Calculated from the integration values in ^{19}F NMR or ^{1}H NMR spectrum. [c] Naphthalene potassium as initiator. [d] 1,1-Diphenyl-3-methylpentyllithium as initiator. [e] 1,1-Diphenyl-3-methylpentyllithium as initiator, in the presence of LiCl.

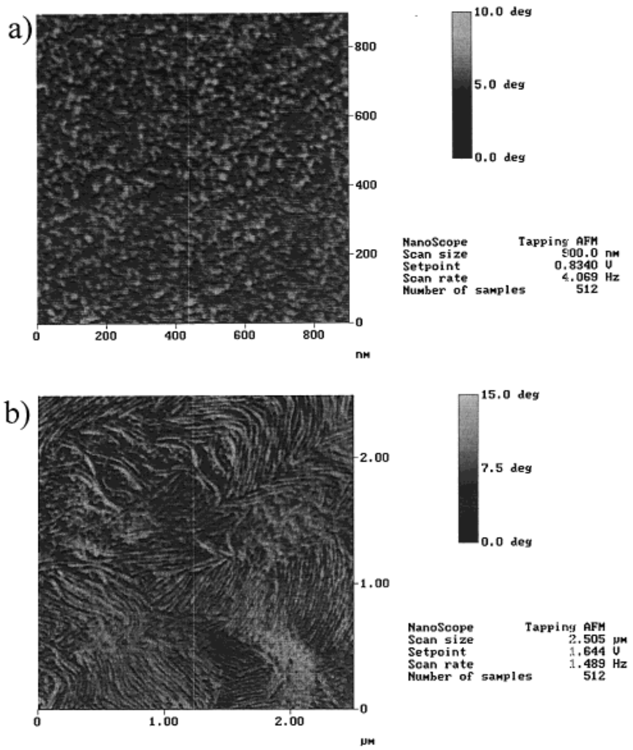

Figure 2. AFM phase-contrast mode measurements of a Tri-7 film cast from (a) tetrahydrofuran and (b) 2,2,3,3-tetrafluoro-1-propanol.

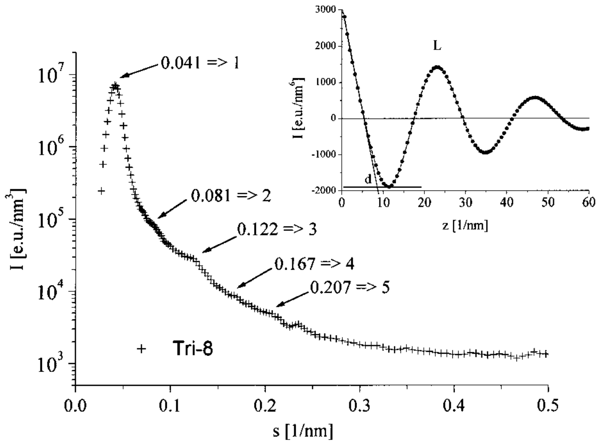

Figure 3. Desmeared intensity distribution of a SAXS measurement on Tri-7. The inset shows the one-dimensional correlation function.

This can be done by atomic force microscopy (AFM) as demonstrated in Figure 2.

Figure 2a shows the morphology of a thin film of the triblock copolymer Tri-7 after slow evaporation of tetrahydrofuran (THF). The phase contrast mode is employed. There is a microphase separation but the phases do not appear very well ordered. Also, thermal annealing above the glass transition does not yield a more perfect structure. A better order can be achieved by using 2,2,3,3-tetrafluoro-1-propanol (TFP) as a solvent. Obviously this is due to the fact that TFP is a more selective solvent for the block with the perfluoroalkyl side chain. Thus the FMA block collapses during the evaporation of the solvent and the lamellar morphology appears well-ordered. It is a frequently observed phenomenon that using very selective solvents leads to a better order in cast block copolymer films.[42] Since the block copolymer Tri-7 is nearly symmetric, it is also reasonable that a lamellar morphology is formed. The obtained lengths are about 30 nm for the long period and 13 nm for the lamella thickness. This is comparable with the results obtained by small-angle X-ray scattering as shown in Figure 3.

The SAXS trace has a first-order maximum at $s^* = 0.041$ nm^{-1}. Higher order maxima occur at multiples of s^*. Thus it is definitively demonstrated that a lamellar order is also achieved in bulk samples that are cooled from the melt. The inset shows the calculated correlation function. The long period L is obtained to be 23 nm and the lamella thickness is about 10 ± 1 nm. As the correlation function shows no plateau at the first minimum, the determination of the lamella thickness has a larger error.

For generating water-soluble block copolymers, the ester splitting is performed at 200 °C for 2 h under vacuum.[43] Finally, the cleavage of the anhydride is done in 1 N NaOH under reflux (compare Figure 1). The reaction can be followed by FT-IR spectroscopy[44] as shown in Figure 4.

In Figure 4a the IR spectra of Tri-7 before and after (dotted line) the ester splitting are depicted. The absorption band at 1720 cm^{-1}, which belongs to the ester carbonyl, vanishes and some significant peaks appear

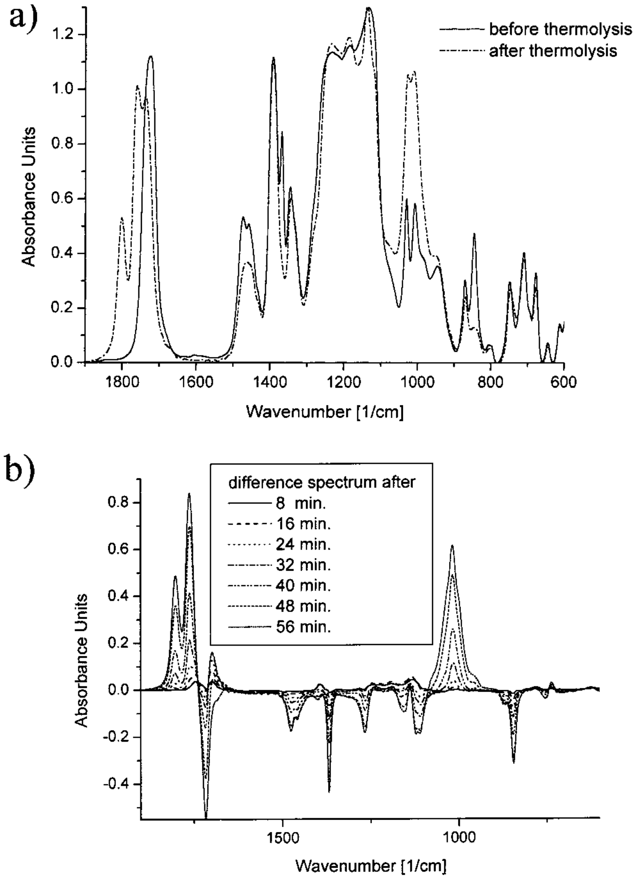

Figure 4. (a) FT-IR spectra of Tri-7 isothermally annealed in a vacuum at 200 °C. The spectra are taken before and after 2 h of annealing. (b) FT-IR difference spectra of Tri-7 for time intervals of 8 min during annealing.

at 1010 (C−O−C), 1760, and 1800 cm^{-1} (C=O) due to the anhydride.[45] In Figure 4b the changes in the spectra in time intervals of 8 min during the ester splitting at 200 °C are shown. From each measurement the first spectrum taken at 0 min was subtracted so the peaks growing toward negative *y*-values are caused by vanishing bands while the opposite peaks are related to growing signals. Isothermal measurements for 2 h at 200 °C on the PFMA homopolymers demonstrate that the ester splitting does not occur for the ester group with the perfluorobutyl side chain. The received spectra are identical prior and after isothermal annealing. This result was confirmed by thermogravimetric measurements, which are not shown here.[46]

After the ester splitting procedure, the polymers with 10 mol % FMA or less were soluble in water. Thus it is shown that hydrophobically modified polymers can be synthesized by the anionic block copolymerization of tBMA and FMA followed by selective ester splitting at 200 °C. The solubility of the polymers is an indication that no cross-linking occurs after heating at 200 °C and alkaline treatment. For the water-soluble species we use the codes given in Table 1 but we add an H in order to make clear that the converted samples are under consideration [e.g., Tri-4H means a triblock copolymer with a middle block of the water soluble sodium salt of the poly(methacrylic acid) converted from sample Tri-4]. The micelle formation behavior of the block copolymers is studied by surface tension measurements as demonstrated in Figure 5.

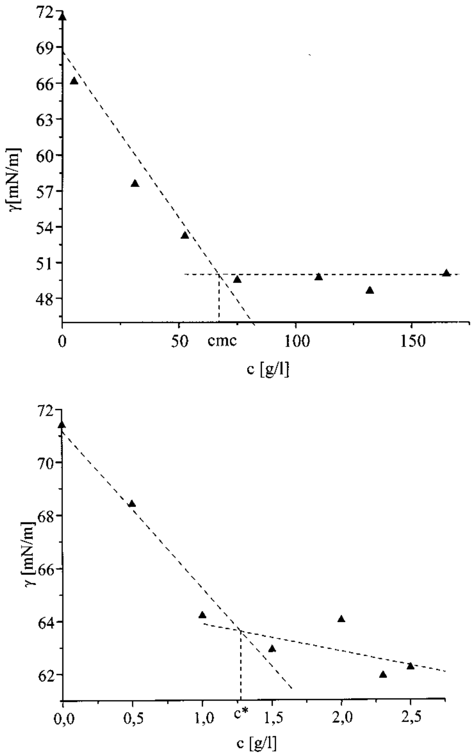

Figure 5. Surface tension of block copolymers (a, top panel) Di-1H and (b, bottom panel) Tri-3H dissolved in water at room temperature.

Figure 5a shows the decrease of the surface tension of water with increasing amount of the diblock copolymer Di-1H. This is the classical behavior and the concentration where the surface tension stays constant with increasing amount of block copolymer in water is called the critical micelle concentration (cmc). For this block copolymer the cmc value at room temperature is 67 g/L. This situation is slightly different for the triblock copolymer Tri-3H (see Figure 5b). The surface tension decreases at much lower concentrations compared to the values from the measurements at the diblock copolymer solutions. Then the surface tension decreases further after reaching a critical value *c**. In this case *c** is at 1.3 g/L. This is an indication that the free energy for the formation of micelles and the free energy for the amphiphilic molecules to cover the free surface is of a very similar order of magnitude. For concentrations of more than 2.5 g/L the solution of the triblock copolymer gets highly viscous and the gel formation dominates the properties. This seems to be more relevant to triblock copolymers. For diblock copolymers it is obvious that in a first step the free surface is covered and then the micelles are formed. The measurements of the reduced viscosities for the polymers are depicted in Figure 6.

The interaction between the hydrophobic fluorinated groups should increase the tendency for clustering and gel formation.[47] For diblock copolymers the formation of micelles should dominate a wide range of concentration, whereas for triblock copolymers an aggregation of the micelles occurs.[48] In Figure 6a the reduced viscosity for the sodium salt of poly(methacrylic acid) without fluorinated blocks (PtBMA-2H) in water is depicted. The polyelectrolyte effect at small concentrations leads to a decrease of the reduced viscosity with increasing concentration followed by a small increase at high concentrations. The behavior of the triblock copolymers is

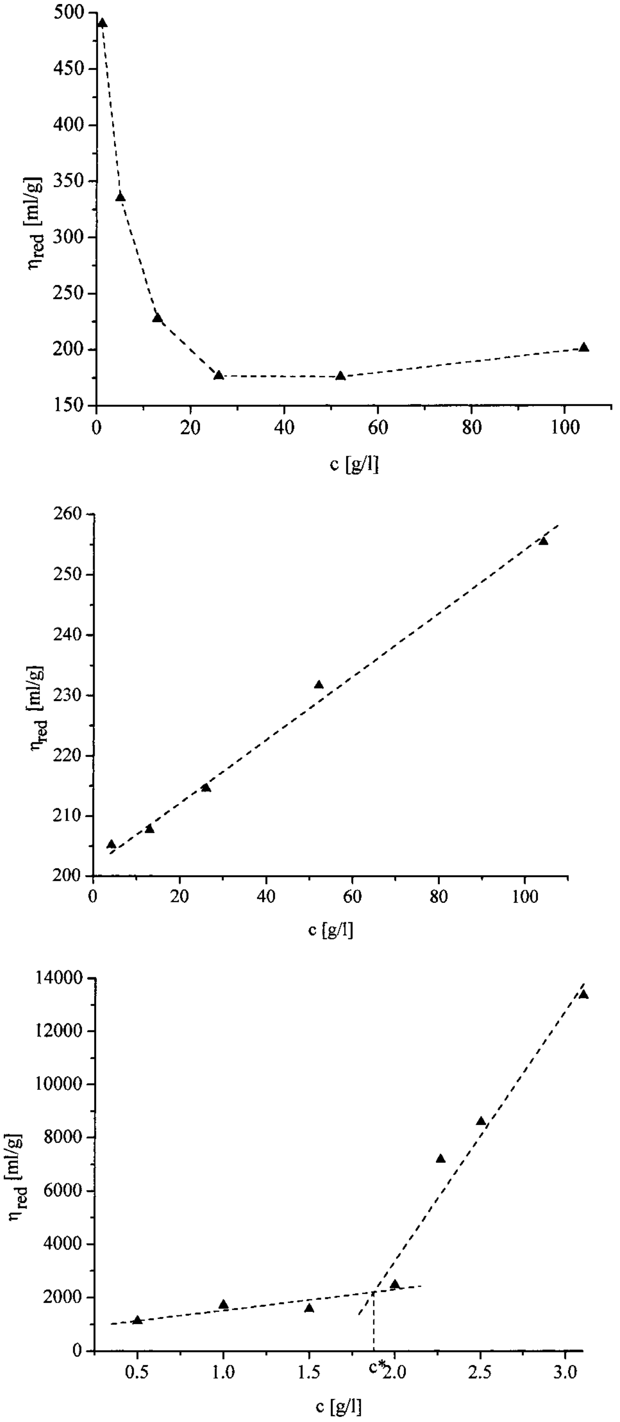

Figure 6. Reduced viscosity (η_{red}) at 25 °C for solutions of (a, top panel) PtBMA-2H, (b, middle panel) Tri-1H, and (c, bottom panel) Tri-3H.

totally different (see Figure 6b). The polyelectrolyte effect at small concentrations cannot be observed. The solution of Tri-1H with 1 mol % FMA shows a linear increase in the reduced viscosity for the concentrations between 4 and 100 g/L. A drastic increase in the reduced viscosity appears for the solution of Tri-3H in water as demonstrated in Figure 6c. Even at very low concentrations η_{red} is about 5 times higher than that of the 1 mol % FMA sample. At a critical concentration of Tri-3H in water of $c^*=1.9$ g/L there is a further change in the behavior. The slope of the curve increases once again and the solution becomes more and more like a gel. The obtained value of c^* coincides with results for the overlap concentration of other polymers.[6] It is assumed that below c^* single chains and micelles are dominating, whereas above c^* the cross-linking of micelles and the gel formation start.[49] The investigation of micellar structures is therefore done at concentrations near c^*. The measurements of Tri-2H (not depicted here) show the same linear increase as shown for Tri-1H but at lower concentrations and higher viscosity. With dynamic light scattering it is possible to determine the size of the micelles as can be seen in Figure 7. In addition the covering of colloidal gold particles by triblock copolymers can be observed.

An aqueous solution of Tri-4H filtered through a 5 μm Millipore filter and colloidal gold were used for DLS measurements. The diluted samples were (a) 6.5×10^{-4} wt % colloidal gold in water, (b) 0.26 wt % of Tri-4H, and (c) a solution with 4.5×10^{-4} wt % colloidal gold and 0.18 wt % Tri-4H. The samples were measured some minutes after preparation. Then sample c was put for 30 min in an ultrasonic bath and kept for some minutes before measuring again (d). The hydrodynamic radius of colloidal gold particles is determined *to* $r_{hyd} =$ 9 nm. The hydrodynamic radius of micelles in sample b is much larger with approximately 70 nm. When both materials are put together in one sample without destroying the already formed micellar structure, the intensity fraction distribution of the hydrodynamic radius shows two peaks close to the radii distributions of the pure components (c). Caused by the fitting procedure (CONTIN[50]), the mean value of the peaks has a larger scattering, but two peaks with nearly the same intensity are always distinguished. Treating the sample with ultrasound, the polymer micelles will be affected. The intensity fraction distribution of the hydrodynamic radius obtained from sample d shows clearly a decrease of larger clusters while the other peak now appears with an increased radius of about 22 nm. The necessity of an ultrasound treatment indicates the stability of the micelles. The size of the colloidal gold particles (a) and of the micelles (b) can be confirmed by SAXS as depicted in Figure 8.

The background-corrected and desmeared intensity distributions from SAXS measurements in Figure 8 are used to calculate the shape and size of the scattering particles. The scattering profile of the colloidal gold particles depicted in Figure 8a can be approximated by that of a sphere[51] with a radius $r = 9.5$ nm, which corresponds with the hydrodynamic radius from the light scattering experiment. In the case of a solution of 0.26 wt % Tri-4H (Figure 8b) in water, a good approximation of the scattering profile can be reached by assuming a spherical core shell structure with an inner radius of 6 nm and an outer radius of 72 nm. It can be assumed that the hydrophobic end blocks of FMA are concentrated in the core of the micelle whereas the swollen hydrophilic middle block of the sodium salt of methacrylic acid builds the shell. Therefore, the measured hydrodynamic radius from light scattering corresponds to the size of the whole micelle. The detected core of the micelle consists of the hydrophobic parts of the triblock copolymers, as can be confirmed by TEM micrographs shown in Figure 9. SAXS measurements of the gold colloid covered with the polymer are dominated by the scattering of the gold core; the shell structure cannot be dissolved.

Figure 9a shows a typical micelle. The micelles are transferred from a solution in water onto a carbon film.

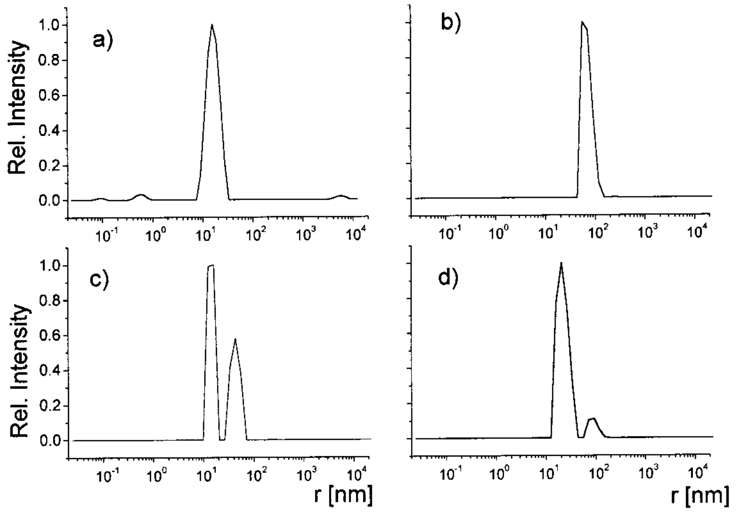

Figure 7. Dilute samples used for dynamic light scattering: (a) 6.5 × 10^{-4} wt % gold colloid in water, (b) 0.26 wt % of Tri-4H, and (c) a solution with 4.5 × 10^{-4} wt % gold colloid and 0.18 wt % Tri-4H. The samples are measured some minutes after preparation. Then sample c was put for 30 min in an ultrasonic bath and kept for some minutes before being measured again (d).

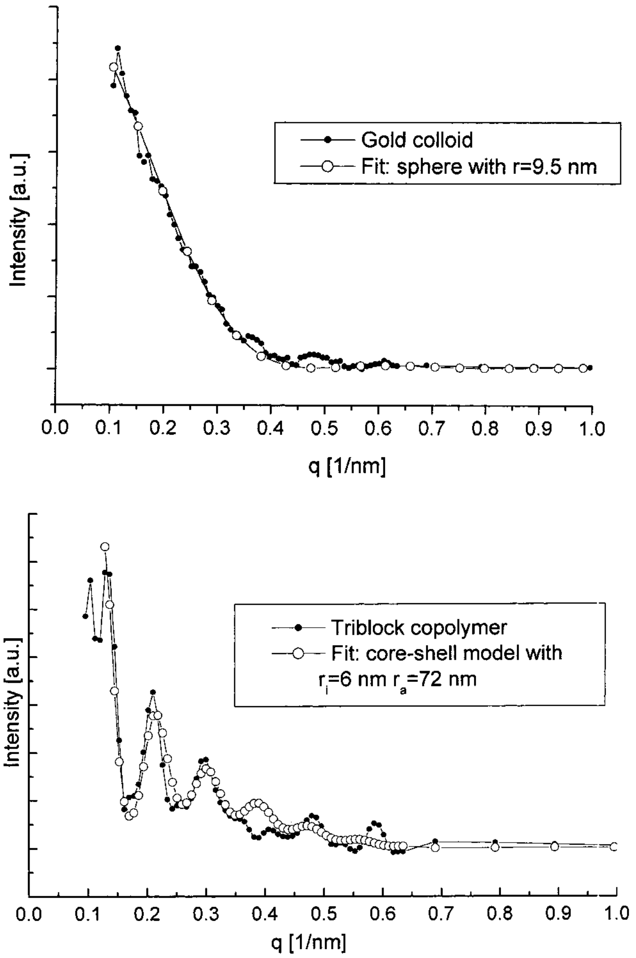

Figure 8. SAXS measurements of (a, top panel) gold colloid (0.013 wt % solution) and (b, bottom panel) solution with 0.26 wt % Tri-4H and approximation (a) with a spherical scatterer and (b) with a spherical core–shell model.

The samples are not stained for TEM. The dark part is the fluorine-containing block due to its larger electron density compared to the other block.[52] When colloidal gold particles are present (see Figure 9b) they are surrounded by the block copolymer after ultrasonic treatment. It is obvious that the hydrophobic block is

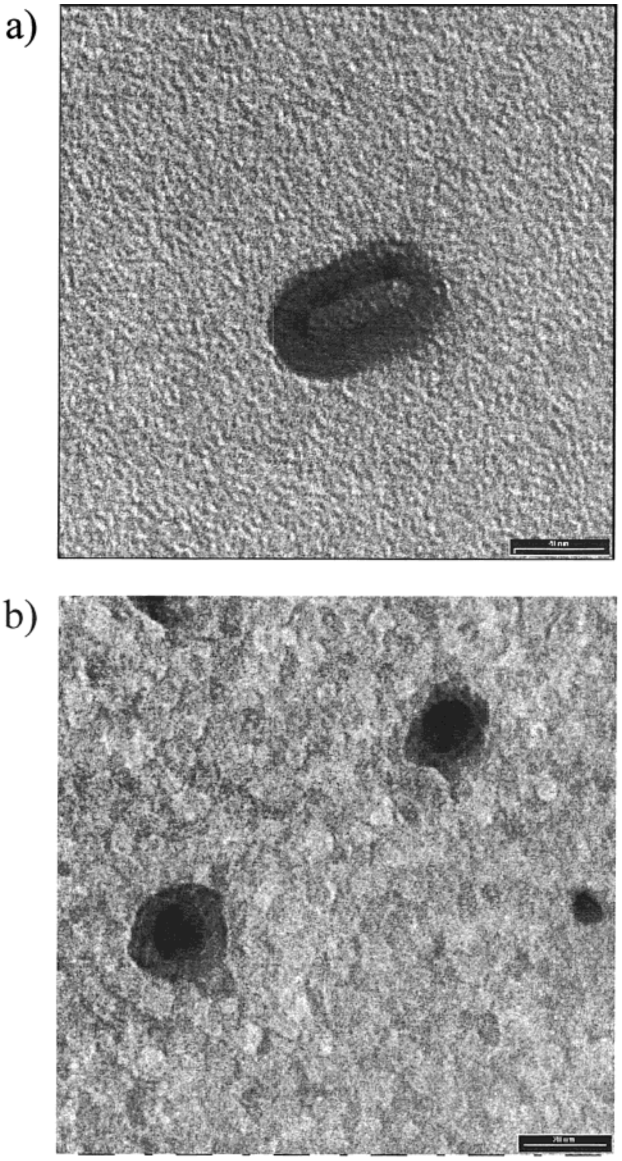

Figure 9. TEM pictures of micelles that are transferred from a solution in water onto a carbon film. The scale bars at the bottom are 20 nm. A micelle of Tri-4H (a) and gold colloid (black particles) covered with Tri-4H (b) are depicted.

attached to the gold particles (the intermediate gray value). The effect of covering gold particles by amphiphilic block copolymers is well-known and is used for the formation of nanoparticles.[53]

Conclusion

The anionically polymerized di- and triblock copolymers of *tert*-butyl methacrylate (tBMA) and 2-(*N*-methylperfluorobutanesulfonamido)ethyl methacrylate (FMA) show a microphase separation in bulk as expected for block copolymers of this kind. The polymers were characterized by SEC and NMR. The water-soluble species are obtained by the ester cleavage producing inter- and intramolecular anhydrides, which can be transformed into sodium methacrylate units in 1 N NaOH under reflux. The thermal ester splitting of the tBMA block at 200 °C does not influence the FMA block. The obtained polymers were soluble in water when the FMA content was below 10 mol %. The polymers with a higher content of FMA do not form a water-soluble species.

For the solutions a critical concentration c^* is determined from surface tension measurements. For triblock copolymers c^* is about 2 g/L, very low compared to the 67 g/L of the diblock copolymers. The existence of micelles at this concentration can be confirmed by light scattering and SAXS. The size of the micelles and their inner structure can be measured additionally by TEM. The possibility of covering gold particles by the triblock copolymers is verified by light scattering and TEM.

Acknowledgment. We thank J. Zimmermann for FT-IR measurements, R. Adhikari for doing the AFM, and R. Thomann for doing the TEM measurements. We acknowledge for financial support the Deutsche Forschungsgemeinschaft (DFG, Graduiertenkolleg Heterogene Polymere), the Bundesministerium für Bildung und Forschung (BMBF, Project 03KRE3HW), and the Fonds der Chemischen Industrie.

References and Notes

(1) Kennedy, J. P. *Pure Appl. Chem.* **1994**, *A31* (11), 1771.
(2) Antonietti, M.; Oestreich, S. *Fluoropolymers* **1999**, *1*, 151.
(3) Forster, S.; Antonietti, M. *Adv. Mater.* **1998**, *10* (3), 195.
(4) Antonietti, M. *Amphiphilic polymers for shaping nanoparticles.* In *Fortschr.-Ber. VDI, Reihe 5* **2000**, *588*, 10.
(5) Fischer, A.; Brembilla, A.; Lochon, P. *Polymer* **2001**, *42* (4), 1441.
(6) Petit, F.; Iliopoulos, I.; Audebert, R.; Szonyi, S. *Langmuir* **1997**, *13*, 4229.
(7) Petit, F.; Iliopoulos, I.; Audebert, R. *J. Chim. Phys.* **1996**, *93*, 887.
(8) Chen, J.; Jiang, M.; Zhang, Y.; Zhou, H. *Macromolecules* **1999**, *32*, 4861.
(9) Zhang, Y.; Li, M.; Fang, Q.; Zhang, Y. X.; Jiang, M.; Wu, C. *Macromolecules* **1998**, *31*, 2527.
(10) Chassenieux, C.; Nicolai, T.; Durand, D. *Macromolecules* **1997**, *30*, 4952.
(11) Xie, X.; Hogen-Esch, T. E. *Macromolecules* **1996**, *29*, 1734.
(12) Hillmyer, M. A.; Bates, F. S. *Macromolecules* **1996**, *29*, 6994.
(13) Ruckenstein, E.; Zhang, H. *Macromolecules* **1998**, *31*, 9127.
(14) Baines, F. L.; Armes, S. P.; Billingham, N. C.; Tucar, T. *Macromolecules* **1996**, *29*, 8151.
(15) Su, T. J.; Styrkas, D. A.; Thomas, R. K.; Baines, F. L.; Billingham N. C.; Armes, S. P. *Macromolecules* **1996**, *29*, 6892.
(16) Patrickios, C. S.; Forder, C.; Armes, S. P.; Billingham, N. C. *J. Polym. Sci., Part A: Polym. Chem.* **1996**, *34*, 1529.
(17) Forder, C.; Armes, S. P.; Billingham, N. C. *Polym. Bull.* **1995**, *35*, 291.
(18) Matsumoto, K.; Kubota, M.; Matsuoka, H.; Yamaoka, H. *Macromolecules* **1999**, *32*, 7122.
(19) Moffitt, M.; Khougaz, K.; Eisenberg, A. *Acc. Chem. Res.* **1996**, *29*, 95.
(20) Klucker, R.; Munch, J. P.; Schosseler, F. *Macromolecules* **1997**, *30*, 3839.
(21) Zhang, Y.; Wu, C.; Fang, Q.; Zhang, Y. X. *Macromolecules* **1996**, *29*, 2494.
(22) Miyamoto, M.; Aoi, K.; Saegusa, T. *Macromolecules* **1989**, *22*, 3540.
(23) Yang, S.; Wang, J.; Ogino, K.; Sundararajan, N.; Ober, C. K. *Polym. Prepr.* **1999**, *40* (1), 416.
(24) Yang, S.; Wang, J.; Ogino, K.; Valiyavettil, S.; Ober, C. K. *Chem. Mater.* **2000**, *12* (1), 33.
(25) Leibler, L.; Orland, H.; Wheeler, J. C. *J. Chem. Phys.* **1983**, *79* (7), 3550.
(26) Chu, B. *Langmuir* **1995**, *11*, 414.
(27) Alexandridis, P. *Curr. Opin. Colloid Interface Sci.* **1996**, *1*, 490.
(28) (a) Mysels, K. J.; Mukerjee, P. *Pure Appl. Chem.* **1979**, *51*, 1085. (b) Everett, D. H. *Pure Appl. Chem.* **1972**, *31* (4), 577.
(29) Robson, R. J.; Dennis, E. A. *J. Phys. Chem.* **1977**, *81* (11), 1075.
(30) Brown, W.; Pu, Z.; Rymden, R. *J. Phys. Chem.* **1988**, *92*, 6086.
(31) Nakano, M.; Matsuoka, H.; Yamaoka, H.; Poppe, A.; Richter, D. *Macromolecules* **1999**, *32*, 697.
(32) Nguyen-Misra, M.; Mattice, W. L. *Macromolecules* **1995**, *28*, 1444.
(33) Semenov, A. N.; Joanny, J.-F.; Khokhlov, A. R. *Macromolecules* **1995**, *28*, 1066.
(34) Varshney, S. K.; Gao, Z.; Zhong, X. F.; Eisenberg, A. *Macromolecules* **1994**, *27*, 1076.
(35) Allen, R. D.; Long, T. E.; McGrath, J. E. *Polym. Bull. (Berlin)* **1986**, *15*, 127.
(36) Smid, J. *J. Am. Chem. Soc.* **1965**, *87* (3), 655.
(37) Wang, J.-S.; Bayard, Ph.; Jerome, R.; Varshney, S. K.; Teyssié, Ph. *Macromol. Symp.* **1995**, *98*, 171.
(38) Lai, J. H. *Macromolecules* **1984**, *17*, 1010.
(39) Strobl, G. R. *Acta Crystallogr.* **1970**, *A26*, 367.
(40) Strobl, G. *The physics of polymers;* Springer: Berlin, 1997.
(41) Andrews, G. D.; Melby, L. R. *Polym. Sci. Technol.* **1985**, *25*, 357.
(42) Sakurai, S. *Trends Polym. Sci.* **1995**, *3* (3), 90.
(43) Guegan, P.; Cernohous, J. J.; Khandpur, A. K.; Hoye, T. R.; Macosko, C. W. *Macromolecules* **1996**, *29*, 4605.
(44) (a) Arndt, K.-F.; Richter, A.; Ludwig, S.; Zimmermann, J.; Kressler, J.; Kuckling, D.; Adler, H.-J. *Acta Polym.* **1999**, *50*, 383−390. (b) Schäfer, R.; Zimmermann, J.; Kressler, J.; Mülhaupt, R. *Polymer* **1997**, *38*, 3745.
(45) Hesse, M.; Meier, H.; Zeeh, B. *Spektroskopische Methoden in der organischen Chemie*; Thieme: Stuttgart and New York, 1991.
(46) van Eck, D. Ph.D. Thesis, Martin-Luther-University Halle-Wittenberg, Halle, Germany, 2000.
(47) Annable, T.; Buscall, R.; Ettelaie, R.; Whittlestone, D. *J. Rheol.* **1993**, *37* (4), 695.
(48) Raspaud, E.; Lairez, D.; Adam, M.; Carton, J.-P. *Macromolecules* **1994**, *27*, 1956.
(49) Liu, Y. C.; Chen, S.-H. Analysis of the Structure, Interaction, and Viscosity of Pluronic Micelles in Aqueous Solutions by Combined Neutron and Light Scattering. In *Scattering from Polymers*; Cebe, P., Hsiao, B. S., Lohse, D. J., Eds.; ACS Symposium Series 739; American Chemical Society: Washington, DC, 2000.
(50) Provencher, S. W. *Comput. Phys. Commun.* **1982**, *27*, 229.
(51) Guinier, A. *X-ray diffraction in crystals, imperfect crystals, and amorphous bodies*; Dover Publications: Mineola, NY, 1994.
(52) van Eck, D.; Höring, S.; Kressler, J.; Arends, P.; Thomann, R. *Polym. Prepr. (Am. Chem. Soc., Polym. Chem.)* **2000**, *41* (1)**,** 726.
(53) Fendler, J. H. (Ed.) *Nanoparticles and nanostructured films*; Wiley-VCH: Weinheim, Germany, 1998.

MA0116809